Published OnlineFirst December 13, 2017; DOI: 10.1158/1535-7163.MCT-17-0006

Small Molecule Therapeutics

Molecular Cancer Therapeutics

Inhibiting Nuclear Phospho-Progesterone Receptor Enhances Antitumor Activity of Onapristone in Uterine Cancer

Yan Huang[1], Wei Hu[1], Jie Huang[1], Fangrong Shen[1], Yunjie Sun[1], Cristina Ivan[2], Sunila Pradeep[1], Robert Dood[1], Monika Haemmerle[1], Dahai Jiang[2], Lingegowda S. Mangala[1], Kyunghee Noh[1], Jean M. Hansen[1], Heather J. Dalton[1], Rebecca A. Previs[1], Archana S. Nagaraja[1], Michael McGuire[1], Nicholas B. Jennings[1], Russell Broaddus[3], Robert L. Coleman[1], and Anil K. Sood[1,2,4]

Abstract

Although progesterone receptor (PR)–targeted therapies are modestly active in patients with uterine cancer, their underlying molecular mechanisms are not well understood. The clinical use of such therapies is limited because of the lack of biomarkers that predict response to PR agonists (progestins) or PR antagonists (onapristone). Thus, understanding the underlying molecular mechanisms of action will provide an advance in developing novel combination therapies for cancer patients. Nuclear translocation of PR has been reported to be ligand-dependent or -independent. Here, we identified that onapristone, a PR antagonist, inhibited nuclear translocation of ligand-dependent or -independent (EGF) phospho-PR (S294), whereas trametinib inhibited nuclear translocation of EGF-induced phospho-PR (S294). Using orthotopic mouse models of uterine cancer, we demonstrated that the combination of onapristone and trametinib results in superior antitumor effects in uterine cancer models compared with either monotherapy. These synergistic effects are, in part, mediated through inhibiting the nuclear translocation of EGF-induced PR phosphorylation in uterine cancer cells. Targeting MAPK-dependent PR activation with onapristone and trametinib significantly inhibited tumor growth in preclinical uterine cancer models and is worthy of further clinical investigation. *Mol Cancer Ther; 17(2); 464–73. ©2017 AACR.*

Introduction

Uterine cancer is the fourth most common malignancy in women and the most common gynecologic cancer in the United States (1). Despite the availability of systemic treatments, including endocrine therapy and combination chemotherapy, patients with recurrent or metastatic uterine cancer have a poor prognosis (2). Progesterone receptor (PR)-targeted therapies are modestly active in patients with uterine cancer, but the underlying molecular mechanisms of PR-targeted therapies are not well understood (3, 4). In the normal endometrium, estrogen drives proliferation of the endometrial glandular epithelium, whereas progesterone counteracts the effects of estrogen. Progesterone acts by binding to the PR and has a dual role through both genomic and nongenomic pathways (5, 6). In humans, the PR gene is expressed as two distinct isoforms of PRA and PRB (7). The PR phosphorylation sites are separated into two groups: basal sites that are phosphorylated in the absence of ligand (Ser 81, Ser 162, Ser 190, Ser 400), and the hormone-dependent sites (Ser 102, Ser 294, and Ser 345; refs. 8, 9). Ligands with agonist or antagonist properties can interact with PR to activate or repress gene expression in target cells (10–12).

Progestins or progesterone agonists (e.g., medroxyprogesterone acetate, norethindrone acetate, and megestrol acetate) block endometrial proliferation (7). Clinical experience would suggest that progestins have better efficacy in tumors that are PR-positive, but these effects are not universal and objective responses, albeit low, are seen in PR-nonexpressing tumor, suggesting other mechanisms of response and resistance are being leveraged (13). Progesterone antagonists exhibit a spectrum of effects ranging from pure antagonists to mixed antagonists. It has been reported that the antagonists RU486 and ZK98299 (onapristone) stimulate PR binding to deoxyribonucleic acid *in vitro* and *in vivo*, but have distinct effects on receptor conformation (10, 14). The mixed antagonist (mifepristone/RU486) with both agonist and antagonist activities may stimulate PR action depending on the cell type, the promoter context, and or the cellular environment of other signaling pathways.

The pure antagonist (onapristone) might be generally incapable of activating transcription and fully antagonizing PR functions

[1]Department of Gynecologic Oncology and Reproductive Medicine, The University of Texas MD Anderson Cancer Center, Houston, Texas. [2]Center for RNA Interference and Non-Coding RNAs, The University of Texas MD Anderson Cancer Center, Houston, Texas. [3]Department of Pathology, The University of Texas MD Anderson Cancer Center, Houston, Texas. [4]Department of Cancer Biology, The University of Texas MD Anderson Cancer Center, Houston, Texas.

Note: Supplementary data for this article are available at Molecular Cancer Therapeutics Online (http://mct.aacrjournals.org/).

Y. Huang and W. Hu contributed equally to this article.

Current address for Y. Huang: Department of Gynecologic Oncology, Fudan University Shanghai Cancer Center, Shanghai, P.R. China; current address for F. Shen, Department of Obstetrics and Gynecology, The First Affiliated Hospital of Soochow University, Suzhou, Jiangsu, P.R. China; and current address for M Haemmerle, Martin-Luther University Halle-Wittenberg, Institute of Pathology, Germany.

Corresponding Author: Anil K. Sood, The University of Texas MD Anderson Cancer Center, 1515 Holcombe Boulevard, Unit 1362, Houston, TX 77030. Phone: 713-745-5266; Fax: 713-792-7586; E-mail: asood@mdanderson.org

doi: 10.1158/1535-7163.MCT-17-0006

Published OnlineFirst December 13, 2017; DOI: 10.1158/1535-7163.MCT-17-0006

(15, 16, 17, 18), and it has demonstrated antitumor activity in breast cancer patients (19). Onapristone is currently under investigation in patients with PR-expressing endometrial tumors (NCT02052128). But, the biological effects and related mechanisms of onapristone in uterine cancer are not well understood.

Here, we evaluated the antitumor activity of onapristone alone and in combination with rationally selected drugs (trametinib) in orthotopic mouse models of uterine cancer and examined their underlying mechanisms of action. We found that the combination of onapristone and trametinib results in superior antitumor effects in uterine cancer models compared with either monotherapy. These effects are, in part, mediated through inhibiting the nuclear translocation of EGF/MAPK–dependent PR activation in uterine cancer cells.

Materials and Methods

Cell cultures

We obtained the uterine and breast cancer cell lines from the MD Anderson Characterized Cell Line Core Facility, which supplies authenticated cell lines. The cell lines were subjected to routine testing to confirm the absence of mycoplasma, and all experiments were performed with cell lines at 60% to 80% confluence. The uterine cancer cell lines KLE, HEC1A, and ISHIKAWA were maintained in specific culture medium, as described previously (20). HEC1B cells were maintained in MEM supplemented with 10% FBS, sodium pyruvate, nonessential amino acids, L-glutamine, and 0.1% gentamicin sulfate (Gemini Bioproducts). SKUT2 cells were maintained in DMEM supplemented with 20% FBS and 0.1% gentamicin sulfate. RL952 cells were maintained in DMEM/F12 supplemented with 20% FBS and 0.1% gentamicin sulfate. The breast cancer cell line T47D was maintained in RPMI1640 supplemented with 10% FBS and 0.1% gentamicin sulfate. For the experiments involving onapristone, the growth medium was replaced with starvation medium, phenol-red-free Opti-MEM (Life Technologies) supplemented with 2% dextran-coated charcoal-stripped serum (HyClone), for 48 hours. EGF treatments were conducted in phenol-red–free Opti-MEM in the absence of serum.

Drugs and antibodies

Onapristone was provided by Arno Therapeutics, Inc. Trametinib (GSK1120212) was purchased from Selleck Chemicals LLC. The antibodies used in Western blotting were phospho-PR (S345), PR (both PRB and PRA, Abcam 32085), p44/42 MAPK, phospho-p44/42 MAPK (Thr202/Tyr204), p21 (all from Cell Signaling Technology), phospho-PR (S294; R&D Systems), and β-actin (Sigma-Aldrich). The antibodies used in immunocytochemistry were phospho-PR (S294; Life Technologies) and phospho-PR (S345; Cell Signaling Technology). The antibodies used in IHC were PR (both PRB and PRA) and phospho-PR (S345; Cell Signaling Technology), p21 (all from Abcam), CD31 (BD Pharmingen), Ki67 (Neomarkers Inc.), cleaved caspase-3 (Biocare Medical LLC), horseradish peroxidase (HRP)–conjugated goat anti-rabbit or anti-mouse immunoglobulin G (Serotec Harlan Bioproducts for Science, Inc.), and Alexa Fluor 594–conjugated anti-rabbit or anti-mouse antibody (Jackson ImmunoResearch Laboratories).

MTT assay

To assess cell survival, cells [ISHIKAWA 3×10^3, HEC1A 5×10^3, SKUT2 3×10^3] were plated in each well of a 96-well plate and maintained overnight in specific culture medium, as described previously (20). Then the growth medium was replaced with phenol-red–free Opti-MEM supplemented with 2% dextran-coated charcoal-stripped serum for 48 hours with or without onapristone or trametinib treatment. Onapristone was dissolved in DMSO with a stock concentration of 0.4 mol/L. The cells were then exposed to onapristone or to trametinib for 72 hours. Controls were treated with an equal volume of vehicle. To assess cell survival, 50 μL of 0.15% MTT (Sigma-Aldrich) was added to each well, and the cells were incubated for 2 hours at 37°C. The medium containing MTT was then removed and 100 μL of dimethyl sulfoxide (Sigma-Aldrich) was added; the cells were then incubated at room temperature for 10 minutes. Absorbance was read at 570 nm using a 96-well Synergy HT-microplate reader (Ceres UV 900C; Bio-Tek Instruments, Inc.). Cell survival was defined as the number of viable cells in the treatment group/number of viable cells in the control group. The IC_{50} concentrations were calculated. Isobologram analysis was performed to evaluate the cytotoxicity of onapristone and trametinib in ISHIKAWA cells using dose–response cell survival curves (16, 20, 21). An interaction index was calculated, as described previously (16, 20, 21). The additive effects (=1), synergistic effects (<1), and antagonistic effects (>1) of the combination of onapristone plus trametinib were determined using the interaction index. The results were analyzed using R (version 2.14.2). The MTT was also performed on the Ishikawa cells after a 72-hour treatment with onapristone at indicated doses, followed by transfection with PR siRNA or control siRNA. PR siRNA and control siRNA (Sigma 00303510, Sigma-Aldrich) transfections were carried out using Lipofectamine 2000 (Invitrogen catalog no. 11668-500).

Western blot analysis

Cell lysates were obtained with RIPA lysis buffer [50 mmol/L Tris-HCl (pH 7.4), 150 mmol/L NaCl, 1% Triton, 0.5% deoxycholate, 2 mmol/L EDTA, and 1 mmol/L sodium orthovanadate) and centrifuged for 15 minutes at 4°C. Protein concentration was then determined using the Bio-Rad Protein Assay Kit (Bio-Rad). Following protein loading (40 μg/well), bands were separated on 8% to 12% gel using SDS-PAGE, transferred to nitrocellulose paper, blocked with 5% BSA for 1 hour at room temperature, and incubated with the primary antibodies overnight at 4°C. The bands were then incubated with HRP–conjugated anti-mouse or anti-rabbit antibodies (GE Healthcare) for 1 hour at room temperature. The blots were developed using an Enhanced Chemiluminescence Detection Kit (Pierce Biotechnology). β-Actin was used for loading control. Densitometry (ImageJ; NIH, Bethesda, MD) was used to assess the differences in the results.

RNA extraction and quantitative real-time PCR

Cells were first homogenized with TRIzol (Invitrogen), and RNA was extracted using Direct-zol RNA MiniPrep (Zymo Research). cDNA was generated with 1 μg of high-quality RNA using a SuperScript-III reverse transcriptase kit (Thermo Scientific). Quantitative real-time PCR was performed in triplicate in an Applied Biosystems 7500 series real-time PCR system, using SYBR Green Master Mix (Thermo Scientific). The 18S rRNA gene was used as an endogenous control. The mean fold change was recorded. The PR primers used were 5′-CGATGCAGTCATTTCTTCCA-3′ (F) and 5′-GTCCTTACCTGTGGGAGCTG-3′ (R). The 18S primers were 5′-CGCCGCTAGAGGTGAAATTC-3′ (F) and 5′-TTGGCAAATGCTTTCGCTC-3′ (R).

Published OnlineFirst December 13, 2017; DOI: 10.1158/1535-7163.MCT-17-0006

Cell proliferation, cell-cycle, and apoptosis assays

To assess cell proliferation, we used the Click-iT EdU Assay Kit (Invitrogen). Cells were seeded into 6-well plates and cultured in a phenol-red–free Opti-MEM with 2% dextran-coated charcoal-stripped serum for 48 hours. Cells were then harvested for the assessment of proliferation after a 96-hour treatment, or apoptosis after a 72-hour treatment, or cell cycle after a 48-hour treatment with 20 μmol/L onapristone and or 100 nmol/L trametinib.

Apoptotic cells were evaluated using an Annexin V apoptosis detection Kit (BD Biosciences). Cell pellets were suspended in 1 mL of 1× Annexin V binding buffer. Following this incubation for 30 minutes, 400 μL of 1× binding buffer was added to each tube, and specimens were analyzed using an XL 4-color flow cytometer.

For cell-cycle analysis, we synchronized the treated cells by maintaining them in serum-free media for 24 hours. The cells were then trypsinized, washed with PBS, fixed in 70% cold ethanol, and stored overnight at 4°C. After washing with PBS, cell pellets were suspended in propidium iodide (Roche Diagnostics) at 50 μg/mL and RNAse A (Qiagen) at 100 μg/mL and incubated in the dark at room temperature. The cell-cycle status was determined using FACS.

IHC and immunofluorescence staining

Paraffin-embedded tumor tissue samples were incubated with Ki67 (1:200), cleaved caspase-3 (1:100), p21 (1:100), or PR (1:140, Abcam 32085) and phospho-PR (S345; 1:100) overnight at 4°C. Antigen retrieval for phospho-PRs (S345) and p21 was performed using 1 mmol/L EDTA-NaOH solution (pH 8.0) by steamer treatment for 30 minutes. Antigen retrieval for total PR was performed using 1× Diva-decloaker by steamer treatment for 20 minutes. Staining with rat monoclonal anti-mouse CD31 (1:800; BD Pharmingen) was performed on the frozen sections. Phospho-PR (S294) or phospho-PR (S345) expression was analyzed using immunofluorescence (IF) staining. Briefly, cells were fixed in 4% paraformaldehyde, permeabilized with 0.025% Triton, incubated with phospho-PR (S294) antibody (1:50) or phospho-PR (S345) antibody (1:50) overnight at 4°C, and then incubated with Alexa Fluor 594–conjugated anti-mouse or anti-rabbit antibody (1:1,000) for 1 hour at room temperature. After washing with PBS, they were incubated with DAPI (Invitrogen) for 10 minutes at room temperature. Mounted samples were visualized using a fluorescent microscope (Leica Microsystems CMS GmbH) with the appropriate filter (original magnification, ×200). For semiquantitative analysis of the expression of phospho-PR (S294) or phospho-PR (S345), or PR, the percentage of positive cells was determined in 6 random 0.159 mm^2 fields at 200× magnification. Two independent investigators evaluated the staining without the knowledge of the parameters.

Animal experiments

Female athymic nude mice (NCr-nu) were purchased from Taconic Farms. All mouse studies were approved by the Institutional Animal Care and Use Committee and the animals were cared for in accordance with guidelines set by the American Association for Accreditation of Laboratory Animal Care and the US Public Health Service Policy on Human Care and Use of Laboratory Animals. For therapeutic experiments, ISHIKAWA uterine cancer cells were directly injected into the uterine horn and to create an orthotopic mouse model of uterine cancer as described previously (20). Forty mice were randomly allocated into 4 treatment groups: control, onapristone (10 mg/kg subcutaneously, dissolving the drug in castor oil containing 10% benzyl benzoate, daily; ref. 22), trametinib (1 mg/kg orally, dissolving the drug in 30% PEG400/0.5% Tween80/5% propylene glycol, daily; ref. 23), or onapristone plus trametinib. Treatment was initiated 2 weeks after cancer cell injection into the uterine horn. After 6 weeks of treatment, the mice were sacrificed, and total body weight, tumor location and weight, and number of tumor nodules were recorded. Tumor specimens were preserved in either optimum cutting temperature medium (Miles Inc.; for frozen slides), or fixed in formalin (for paraffin slides) for further analysis.

Statistical analyses

Statistical analyses were performed using the Statistical Package for Social Science software version 18.0 (SPSS, Inc.). Continuous variables were compared using a Student *t* test (for 2 groups) or ANOVA (for all groups) if the data were normally distributed. For nonparametric distributions, the Mann–Whitney *U* test was used. A P value of <0.05 was deemed statistically significant.

Results

In vitro effects of onapristone in uterine cancer cells

To investigate the biological effects of onapristone in uterine cancer cells, we first examined the mRNA and protein expression of PR in a panel of uterine cancer cell lines and a breast cancer cell line (T47D; Fig. 1A and B). We found that PR was highly expressed at both RNA and protein levels in ISHIKAWA cells, but weakly expressed in SKUT2 cells. We selected the ISHIKAWA, HEC1A, and SKUT2 cell lines based on PR expression and assessed the effects of onapristone on cell survival using the MTT assay. We found that onapristone treatment produced a reduction in the viability of ISHIKAWA cells (Fig. 1C). Furthermore, PR silencing significantly decreased the onapristone sensitivity of the PR-high–expressing Ishikawa cells, compared with control siRNA (**, $P < 0.01$, Supplementary Fig. S1). No significant effects were noted in the other cell lines, suggesting that most of the uterine cancer cell lines are relatively resistant to onapristone (24, 25). Therefore, we selected ISHIKAWA and SKUT2 cells for further *in vitro* and *in vivo* studies. To identify potential mechanisms by which onapristone exerts its antitumor activity, we next tested its effects on proliferation, apoptosis, and cell cycle in ISHIKAWA and SKUT2 cells. Onapristone increased rates of apoptosis (vs. control, $P < 0.01$) in PR-high–expressing cells (ISHIKAWA), but not in PR-weak–expressing cells (SKUT2; Fig. 1D). Onapristone also decreased proliferation in ISHIKAWA cells, but not in SKUT2 cells (Fig. 1E). In addition, onapristone induced G_1-phase arrest in ISHIKAWA cells, but not in SKUT2 cells (Fig. 1F).

It is known that PR is phosphorylated at different sites (basal sites S81, S162, S190, and S400 and hormone-dependent sites S102, S294, and S345), and their ligand-induced phosphorylation has been well characterized (9). Next, we tested the effects of onapristone on PR phosphorylation in uterine cancer cells. Western blot analysis showed that the expression of phospho-PR (S345) in ISHIKAWA cells was significantly inhibited by onapristone in a dose-dependent manner at 24 hours (Fig. 1G). Meanwhile, the expression of the PR-targeted p21 gene (26) was increased in ISHIKAWA cells at 48 and 72 hours, but not detectable in SKUT2 cells at 24, 48, and 72 hours (Fig. 1H). Surprisingly, we also found that onapristone induces slight increase in phosphorylation of p44/42 MAPK in ISHIKAWA cells in a dose-dependent manner, which prompted us to consider that MEK inhibition might enhance the efficacy of onapristone in uterine cancer.

Published OnlineFirst December 13, 2017; DOI: 10.1158/1535-7163.MCT-17-0006

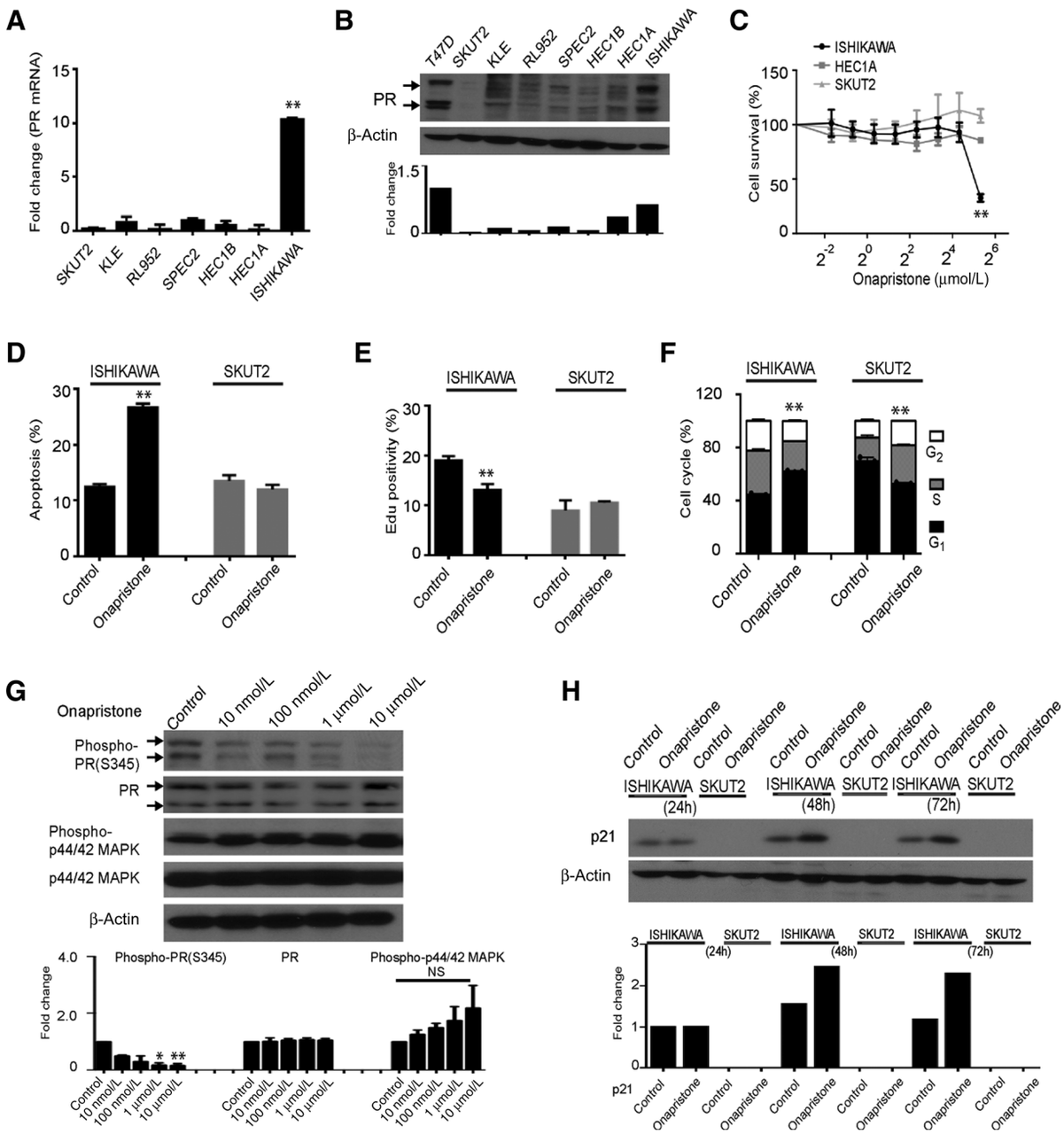

Figure 1.

In vitro effects of onapristone in uterine cancer cells. Real-time PCR (**A**) and Western blot analyses (**B**) of PR expression in a panel of uterine cancer cell lines. **C,** Cell viability after treatment with the indicated concentrations of onapristone for 72 hours. Cell viability was defined as the percentage of viable cells in the treatment group relative to viable cells in the control group. Data represent the means of triplicate measurements with error bars to represent the SEM. **, $P < 0.01$ compared with the control group. *In vitro* functional studies of apoptosis (**D**) for 72 hours, proliferation (**E**) for 96 hours, and cell cycle (**F**) for 48 hours in ISHIKAWA and SKUT2 cells treated with 20 μmol/L onapristone. Data represent the means of triplicate measurements with error bars to represent the SEM. **, $P < 0.01$ **G,** Western blot analysis of phospho-PR (S345) and phospho-p44/42 MAPK expression in ISHIKAWA cells treated with the indicated concentrations of onapristone for 24 hours. Quantification of band intensity relative to phospho-PR intensity is shown graphically. *, $P < 0.05$; **, $P < 0.01$ compared with the control group. Quantification of band intensity relative to p44/42 MAPK intensity is shown graphically. NS indicates $P > 0.05$, compared with the control group. **H,** Western blot analysis of p21 expression in ISHIKAWA and SKUT2 cells treated with 10 μmol/L onapristone for 24, 48, and 72 hours. Quantification of band intensity relative to β-actin intensity is shown graphically.

Published OnlineFirst December 13, 2017; DOI: 10.1158/1535-7163.MCT-17-0006

MEK inhibition enhanced antitumor activity of onapristone in uterine cancer cells

On the basis of our *in vitro* data and the existing knowledge that MAPKs may serve to couple PR protein stability to regulation of transcriptional activity (27), we assessed whether the combination of onapristone and trametinib exerts synergistic or additive effects on uterine cancer cells. We selected trametinib for the *in vitro* and *in vivo* studies because trametinib is already FDA-approved for treating several malignancies. ISHIKAWA and SKUT2 cells were treated with onapristone and trametinib at the indicated doses, as the sensitivity of the uterine cancer cell lines to trametinib is quite different. The MTT assay and isobologram analysis showed a synergistic effect of onapristone and trametinib in the ISHIKAWA cells, but not in SKUT2 cells (Fig. 2 A–C; Supplementary Fig. S2). These results suggest that MEK inhibition enhances the sensitivity of uterine cancer cells to onapristone.

Further *in vitro* studies showed that combination treatment significantly increased rates of apoptosis by 1.7-fold compared with onapristone alone ($P < 0.01$) and 3.2-fold compared with trametinib alone ($P < 0.01$) in ISHIKAWA cells (Fig. 2D). Combination treatment decreased the proliferation rate by 42.7% compared with onapristone alone ($P < 0.01$) and 53.2% compared with trametinib alone ($P < 0.01$) in ISHIKAWA cells (Fig. 2E). Furthermore, the combination treatment increased the proportion of the cell population in the G_1 phase over that observed for onapristone or trametinib alone (Fig. 2F).

***In vivo* effects of onapristone, trametinib, or combination therapy in orthotopic mouse models of uterine cancer**

Next, we tested the effects of the combination therapy in orthotopic mouse models of PR-high–expressing uterine tumors. In the ISHIKAWA model, onapristone demonstrated more antitumor activity than no treatment [65.5% reduction in tumor weight versus control $P < 0.05$] and 63.6% decrease in the number of tumor nodules versus control ($P < 0.01$; Fig. 3A and B). Trametinib treatment also exhibited antitumor activity (86.2% reduction in tumor weight vs. control $P < 0.01$) and 76.0% decrease in the number of tumor nodules versus control ($P < 0.01$; Fig. 3A and B). The combination of both drugs resulted in a large reduction in tumor weight in the ISHIKAWA model (96.5% vs. control; $P < 0.01$) and 85.2% decrease in the number of tumor nodules versus control ($P < 0.01$; Fig. 3A and B). The combination of both drugs resulted in a significant reduction in tumor weight in the ISHIKAWA model, compared with onapristone or trametinib (89.7% vs. onapristone, $P < 0.05$; 74.5% vs. trametinib, $P < 0.05$). The combination of both drugs resulted in a significant reduction in tumor nodules in the ISHIKAWA model, compared with onapristone alone (59.6% vs. onapristone, $P < 0.05$). No obvious toxicity was observed in any of the groups; the mean body weight was similar across all groups (Fig. 3C). No antitumor activity of onapristone was seen in the PR-weak–expressing SKUT2 model (Supplementary Fig. S3).

To examine the biological effects of onapristone–trametinib combination therapy, we examined tumor specimens from the ISHIKAWA mouse model for markers of proliferation (Ki67), apoptosis (cleaved caspase-3), microvessel density (MVD; CD31), phospho-PR (S345), total PR and downstream target of PR (p21). Representative images of IHC staining are presented in Fig. 3D. We observed that rates of apoptosis were significantly increased in the combination group over onapristone or trametinib alone from 7.9 ± 1.1 to 26.6 ± 2.2 ($P < 0.01$); from 11.1 ± 0.7 to 26.6 ± 2.2 ($P < 0.01$). Specifically, expression of cleaved caspase-3

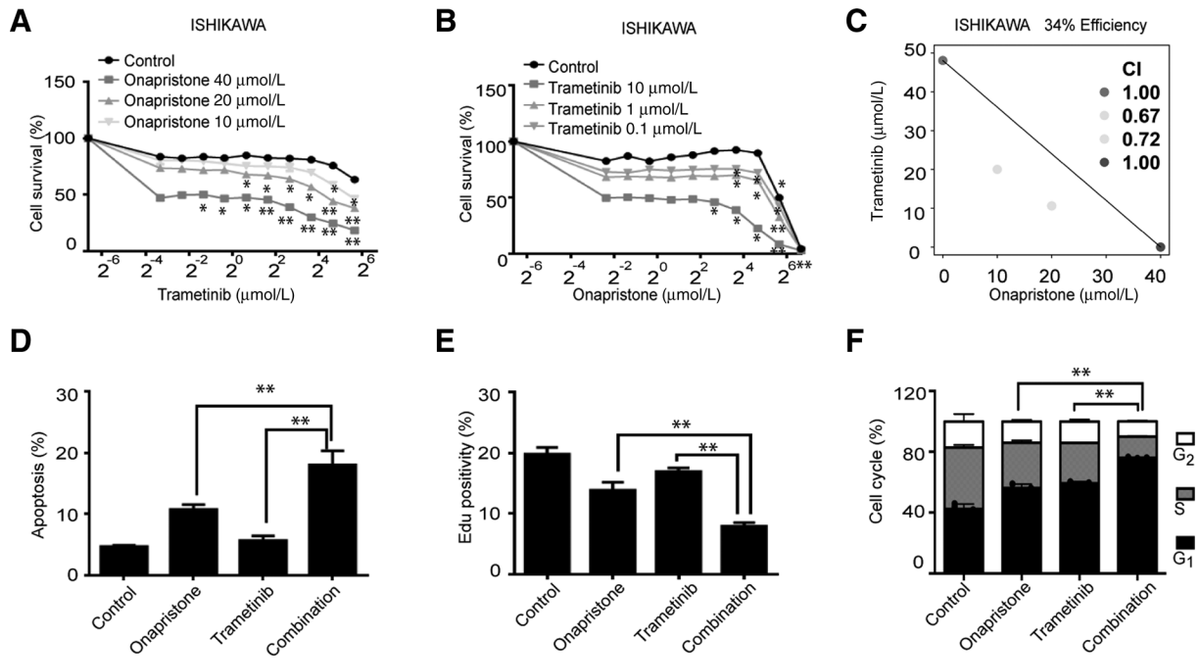

Figure 2.

In vitro effects of onapristone and trametinib in uterine cancer cell lines. **A** and **B**, Cell viability after treatment with onapristone and trametinib at the indicated doses in ISHIKAWA cells for 72 hours. Data represent the means of triplicate measurements with error bars to represent the SEM. *, $P < 0.05$ and **, $P < 0.01$ compared with the control group. **C,** Isobologram analysis of the two-drug interaction in ISHIKAWA cells. *In vitro* functional studies of apoptosis (**D**) for 72 hours, cell proliferation for 96 hours (**E**), and cell cycle (**F**) at 48 hours in ISHIKAWA cells treated with 20 μmol/L onapristone combined with 100 nmol/L trametinib. **, $P < 0.01$ compared with the single drug.

Published OnlineFirst December 13, 2017; DOI: 10.1158/1535-7163.MCT-17-0006

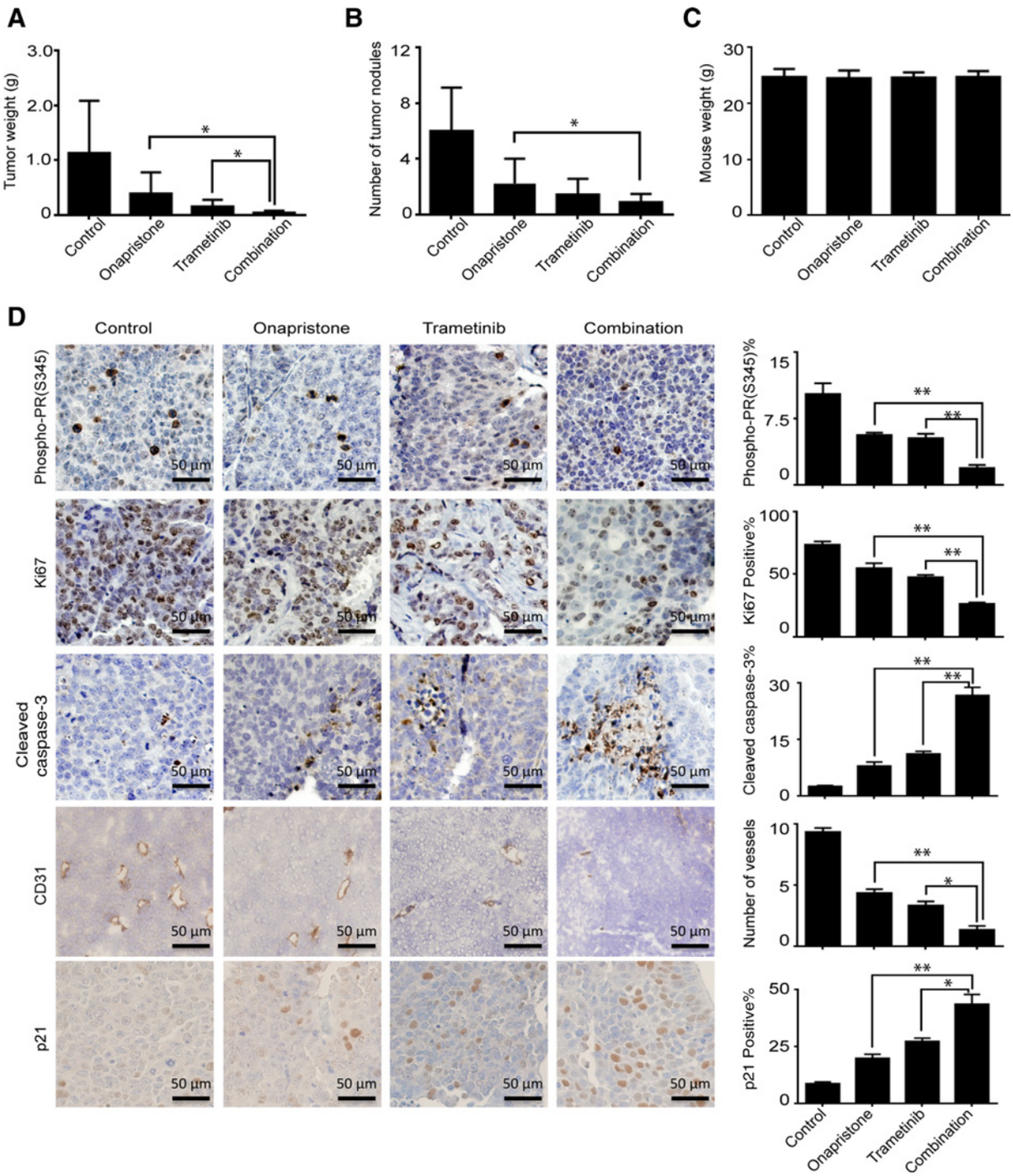

Figure 3.

In vivo effects of onapristone and trametinib in orthotopic mouse model of uterine cancer. *In vivo* effect of onapristone, trametinib, and the combination of both drugs on tumor weight (**A**), number of tumor nodules (**B**), and body weight (**C**). Error bars indicate the SEM; *, $P < 0.05$. **D,** IHC staining showing the effects of onapristone, trametinib, and the combination on apoptosis (cleaved caspase-3), cell proliferation (Ki67), and MVD (CD31) in the ISHIKAWA model. Predictive markers [phospho-PR (S345) and p21] are shown for the ISHIKAWA model. *, $P < 0.05$ and ** $P < 0.01$, compared with the single drug; Original magnification, ×200.

and p21 was increased in the combination treatment group (Fig. 3D), whereas levels of phospho-PR (S345) and Ki67 and CD31 were significantly decreased, but total PR was not significantly changed (Supplementary Fig. S4). These results confirmed our *in vitro* findings that combination treatment showed better antitumor activity than did either monotherapy.

Published OnlineFirst December 13, 2017; DOI: 10.1158/1535-7163.MCT-17-0006

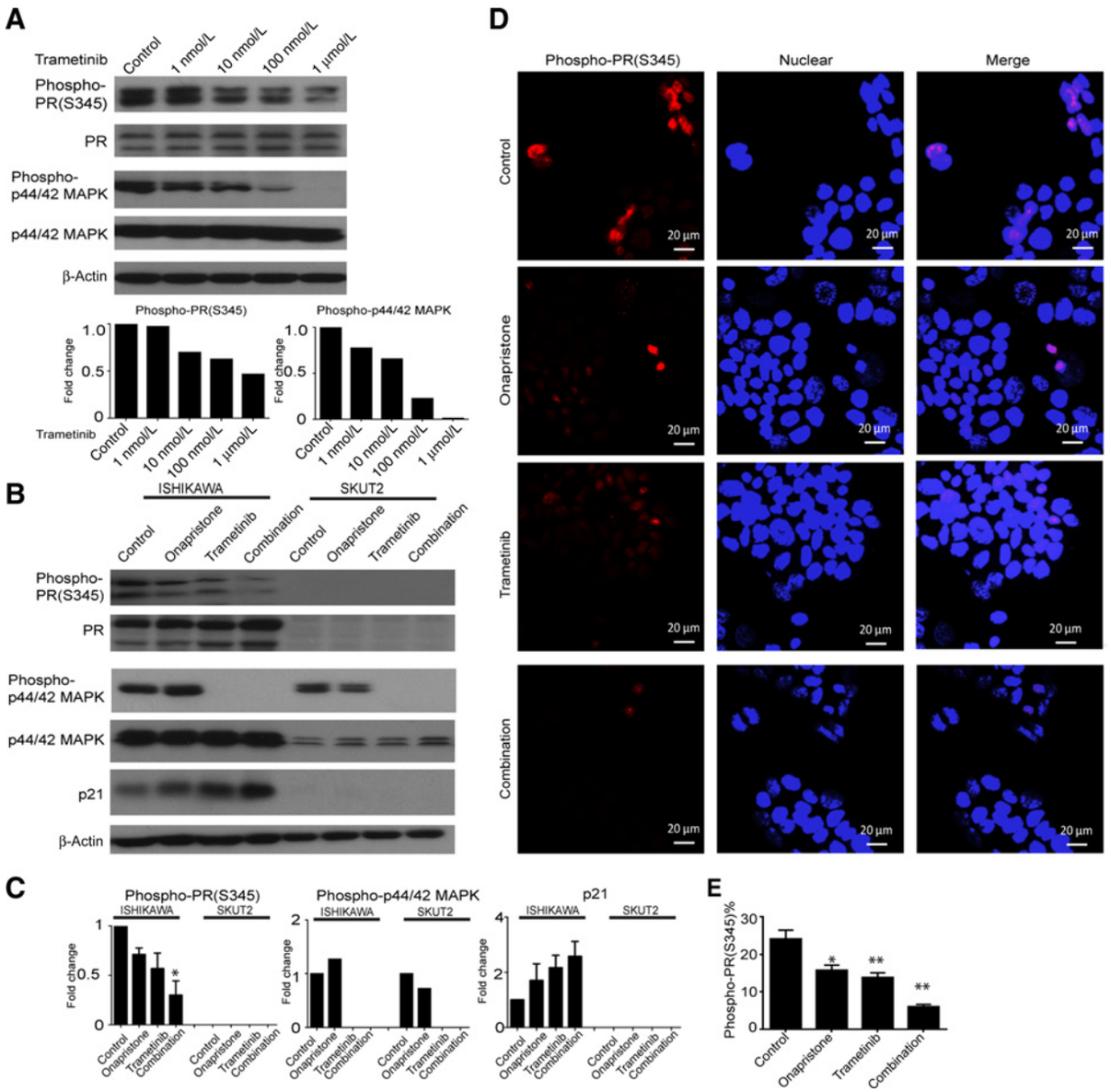

Figure 4.

Effects of onapristone or trametinib on the nuclear translocation of phospho-PR (S345) in uterine cancer cells. **A,** Western blot and semiquantitative analysis of phospho-PR (S345) and phospho-p42/44 MAPK expression in ISHIKAWA cells treated with trametinib at the indicated doses for 24 hours. Western blot (**B**) and semiquantitative analysis (**C**) of phospho-PR(S345) and phospho-p42/44 MAPK expression in ISHIKAWA and SKUT2 cells treated with 10 μmol/L onapristone, 100 nmol/L trametinib, or a combination for 24 hours. *, $P < 0.05$, compared with control. P21 was assessed using 10 μmol/L onapristone, 100 nmol/L trametinib, or a combination for 48 hours ($P > 0.05$, compared with control). IF (**D**) and semiquantitative analysis (**E**) of the nuclear phospho-PR (S345) in ISHIKAWA cells treated with 10 μmol/L onapristone, 100nmol/L trametinib, or a combination for 24 hours. Data represent the means of six random field measurements with error bars to represent SEM. *, $P < 0.05$ and **, $P < 0.01$, compared with the control.

Blocking the nuclear translocation of phospho-PR by trametinib or onapristone or the combination in uterine cancer cells

It has been reported that PR phosphorylation at S345 is also MAPK-dependent (5, 28). We further tested whether trametinib can also inhibit PR phosphorylation at S345. Western blot analysis showed that the expression of phospho-PR (S345) was decreased by trametinib treatment (Fig. 4A). Phosphorylation of p44/42 MAPK was also inhibited by trametinib treatment. Moreover, the combination treatment significantly decreased phospho-PR (S345) expression and increased p21 expression in ISHIKAWA cells compared with the controls (Fig. 4B and C). Furthermore, IF analysis revealed that MEK inhibition enhances the sensitivity of uterine cancer cells to onapristone, likely through blocking the nuclear translocation of phospho-PR (S345; Fig. 4D and E).

In addition, PR phosphorylation at S294 is also MAPK-dependent (29, 30). Because the expression of phospho-PR (S294) in ISHIKAWA cells is low, we used R5020 (PR agonist) to induce it. There are at least two independent mechanisms for nuclear

Published OnlineFirst December 13, 2017; DOI: 10.1158/1535-7163.MCT-17-0006

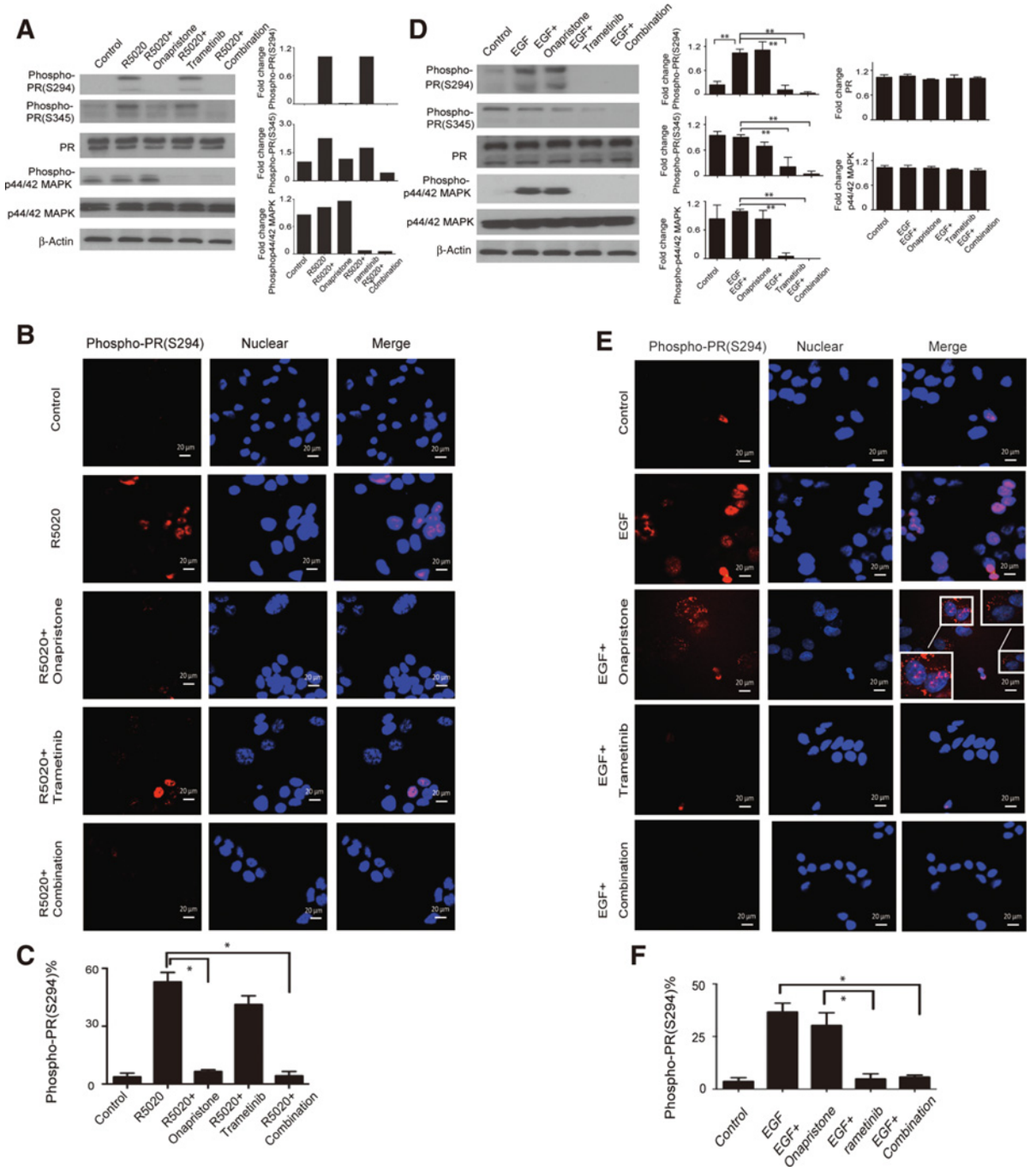

Figure 5.

Effects of onapristone, trametinib, and combination treatment on the nuclear translocation of R5020 or EGF-induced phospho-PR (S294) in uterine cancer cells. **A,** Western blot and semiquantitative analysis of R5020-induced phospho-PR expression in ISHIKAWA cells treated with 10 μmol/L onapristone, 100 nmol/L trametinib, or both for 2 hours, followed by 25 nmol/L R5020 for 1 hour. IF (**B**) and semiquantitative analysis (**C**) of R5020-induced phospho-PR expression and location in ISHIKAWA cells treated with 10 μmol/L onapristone, 100 nmol/L trametinib, or both for 2 hours followed by 25 nmol/L R5020 for 1 hour. Data represent the means of 6 random field measurements with error bars to represent SEM. *, $P < 0.05$, compared with the R5020 treatment. **D,** Western blot and semiquantitative analysis of EGF-induced phospho-PR expression and location in ISHIKAWA cells treated with 10 μmol/L onapristone, 100 nmol/L trametinib, or both for 2 hours, followed by treatment with 30 ng/mL EGF for 30 minutes. **, $P < 0.01$, compared with EGF treatment or control. IF (**E**) and semiquantitative analysis (**F**) of EGF-induced phospho-PR expression and location in ISHIKAWA cells treated with 10 μmol/L onapristone, 100 nmol/L trametinib, or both for 2 hours, followed by treatment with 30 ng/mL EGF for 30 minutes. Data represent the means of six random field measurements with error bars to represent SEM. *, $P < 0.05$, compared with EGF treatment.

Published OnlineFirst December 13, 2017; DOI: 10.1158/1535-7163.MCT-17-0006

translocation of phospho-PR (S294). We first tested whether onapristone inhibits R5020-induced (ligand-dependent) nuclear translocation of phospho-PR (S294). Western blotting and IF showed that treatment of ISHIKAWA cells with R5020 at 25 nmol/L for 1 hour resulted in PR phosphorylation at the S294 site and nuclear translocation, whereas treatment of ISHIKAWA cells with onapristone at 10 μmol/L blocked R5020-induced nuclear translocation of phospho-PR (S294). IF staining with the phospho-antibody reflects a change in cellular location of phospho-PR, because onapristone did not affect total PR protein levels (Fig. 5A–C; Supplementary Fig. S4). Onapristone blocked R5020-induced phospho-PR (S345; Fig. 5A). However, trametinib did not decrease R5020-induced nuclear translocation of phospho-PR (S294) and phospho-PR (S345). In addition, phospho-p44/42 MAPK was blocked by either trametinib or the combination of onapristone and trametinib. It has been reported that MAPKs play a dual role in PR subcellular trafficking and aid the rapid nuclear association of PR via S294 phosphorylation in response to growth factors in the absence of ligand (31). Therefore, we tested whether trametinib can block EGF-mediated (ligand-independent) phospho-PR (S294) nuclear translocation. Western blot and IF analyses revealed that EGF significantly induced phospho-PR (S294) nuclear translocation and that EGF-induced nuclear translocation of phospho-PR (S294) was blocked by trametinib treatment (Fig. 5D–F). Interestingly, IF analysis also revealed that onapristone induced phospho-PR (S294) translocation from a nuclear to a perinuclear location (Fig. 5E). In addition, phospho-p44/42 MAPK was induced by EGF and blocked by either trametinib or the combination of both drugs. Ligand-dependent phospho-PR (S294) blocked by onapristone and ligand-independent phospho-PR (S294) inhibited by trametinib suggests that MEK inhibition enhances the sensitivity of uterine cancer cells to onapristone, likely through blocking the nuclear translocation of phospho-PR (S294). We also found that EGF did not induce phospho-PR (S345; Fig. 5D).

Discussion

The key findings from this study are that the combination therapy of onapristone and trametinib results in superior preclinical antitumor effects in uterine cancer compared with either monotherapy, both *in vitro* and *in vivo*. Although the exact mechanisms by which the combination of onapristone and trametinib exerts its synergistic effects remain largely unknown, we have identified that nuclear translocation of phospho-PR (S294) and phospho-PR (S345) is a key determinant of uterine cancer cells' sensitivity to onapristone and trametinib treatment.

Progesterone acts by binding to PR and regulating genomic and non-genomic pathways in both a ligand-dependent (25) and a ligand-independent manner (5). Our study further indicates that MEK inhibition enhances the sensitivity of uterine cancer cells to onapristone, partially through blocking the nuclear translocation of phospho-PR (S294 and S345). MAPK-dependent activation of phospho-PR might contribute to resistance to ligand-dependent PR targeted therapy. MAPKs have been reported to regulate PR at multiple points, including transcriptional synergy and nuclear translocation and play a dual role in PR subcellular trafficking (31). In the absence of ligand, phosphorylation of PR by MAPKs is likely to aid the rapid nuclear translocation of PR *via* S294 phosphorylation in response to EGF (27, 30). It has also been reported that RU486 with both mixed agonist and antagonist activities induces the PR phosphorylation at S294 to the same extent as R5020 (PR-agonist; ref. 32). In contrast, onapristone blocks the R5020-induced PR phosphorylation at S294 (9). Consistent with those results, our study has shown that EGF-induced nuclear translocation of phospho-PR (S294) was blocked by trametinib or onapristone while R5020-induced nuclear translocation of phospho-PR (S294) was blocked by onapristone. The third possible explanation is that trametinib can inhibit pMAPK induced by onapristone or R5020 or EGF, which may enhance the antitumor activity. Still, the mechanism by which MEK inhibition enhances the sensitivity of uterine cancer cells to onapristone needs to be explored further. The fourth possible explanation for the synergistic effect we observed could be that extracellular rapid activation of the EGF/EGFR and Src/MAPK cascade may promote PR phosphorylation-dependent interactions with other regulatory molecules (coactivators or cosuppressors) and mediate nonclassical transcriptional synergy (p21; refs. 27, 28). Consistent with this possibility, we found that p21 expression was higher in PR-high–expressing cells treated with both onapristone and trametinib compared with either monotherapy. These results provide additional support for the rationale for the use of onapristone-trametinib combination therapy for treatment of uterine cancer.

Identification of biomarkers for predicting response to PR-targeted therapies is important for further clinical development. We have identified that nuclear translocation of phospho-PR (S294) and phospho-PR (S345) is a key determinant of uterine cancer cells' sensitivity to onapristone and trametinib treatment. Consistent with our findings, a recent study showed that patients with uterine cancer with active PR (a transcriptionally active PR) may benefit from progesterone antagonists (24, 25). Whether active PR can be a reliable biomarker to predict onapristone sensitivity will require additional testing (13).

In summary, our studies indicate that nuclear translocation of phospho-PR (S294) and phospho-PR (S345) is a key determinant of uterine cancer cells' sensitivity to onapristone and trametinib treatment. Targeting MAPK-dependent PR activation with onapristone alone or in combination with trametinib, significantly inhibited tumor growth in preclinical uterine cancer models and is worthy of further clinical investigation.

Disclosure of Potential Conflicts of Interest

W. Hu reports receiving a commercial research grant from Arno Therapeutics, Inc. No potential conflicts of interest were disclosed by the other authors.

Authors' Contributions

Conception and design: Y. Huang, W. Hu, A.K. Sood
Development of methodology: Y. Huang, W. Hu, A.K. Sood
Acquisition of data (provided animals, acquired and managed patients, provided facilities, etc.): Y. Huang, S. Pradeep, M. Haemmerle, D. Jiang, K. Noh, J.M. Hansen, H.J. Dalton, R.A. Previs, A.S. Nagaraja, N.B. Jennings, R. Broaddus, A.K. Sood
Analysis and interpretation of data (e.g., statistical analysis, biostatistics, computational analysis): Y. Huang, J. Huang, Y. Sun, C. Ivan, S. Pradeep, M. Haemmerle, M. McGuire, N.B. Jennings, R.L. Coleman, A.K. Sood
Writing, review, and/or revision of the manuscript: Y. Huang, W. Hu, R. Dood, L.S. Mangala, J.M. Hansen, H.J. Dalton, M. McGuire, R. Broaddus, R.L. Coleman, A.K. Sood
Administrative, technical, or material support (i.e., reporting or organizing data, constructing databases): Y. Huang, W. Hu, F. Shen, Y. Sun, S. Pradeep, N.B. Jennings, R. Broaddus, A.K. Sood
Study supervision. Y. Huang, W. Hu, S. Pradeep, A.K. Sood

Acknowledgments

Portions of this work were supported by the NIH (P50 CA083639, P50 CA098258, CA177909; to A.K. Sood), Arno Therapeutics, Inc. (to W. Hu), the Frank McGraw Memorial Chair in Cancer Research (to A.K. Sood), the Ann Rife Cox Chair in Gynecology (to R. Coleman), and the Institutional Core Grant (CA16672) to MD Anderson Cancer Center from the NIH (Bethesda, MD). H.J. Dalton, J.M. Hansen, R.A. Previs, and R. Dood were supported by a T32 Training Grant (T32CA101642; to A.K. Sood) from the National Cancer Institute, the Department of Health and Human Services, and the NIH (Bethesda, MD). We thank Amy Ninetto in the Department of Scientific Publications at the MD Anderson Cancer Center for editing our article. We also thank Arno Therapeutics, Inc. for providing onapristone for preclinical studies.

The costs of publication of this article were defrayed in part by the payment of page charges. This article must therefore be hereby marked *advertisement* in accordance with 18 U.S.C. Section 1734 solely to indicate this fact.

Received January 2, 2017; revised June 19, 2017; accepted November 21, 2017; published OnlineFirst December 13, 2017.

References

1. Siegel RL, Miller KD, Jemal A. Cancer statistics, 2015. CA Cancer J Clin 2015;65:5–29.
2. Temkin SM, Fleming G. Current treatment of metastatic endometrial cancer. Cancer Control 2009;16:38–45.
3. Amant F, Moerman P, Neven P, Timmerman D, Van Limbergen E, Vergote I. Endometrial cancer. Lancet 2005;366:491–505.
4. Dedes KJ, Wetterskog D, Ashworth A, Kaye SB, Reis-Filho JS. Emerging therapeutic targets in endometrial cancer. Nat Rev Clin Oncol 2011;8: 261–71.
5. Hagan CR, Daniel AR, Dressing GE, Lange CA. Role of phosphorylation in progesterone receptor signaling and specificity. Mol Cell Endocrinol 2012;357:43–9.
6. Losel R, Wehling M. Nongenomic actions of steroid hormones. Nat Rev Mol Cell Biol 2003;4:46–56.
7. Yang S, Thiel KW, Leslie KK. Progesterone: the ultimate endometrial tumor suppressor. Trends Endocrinol Metab 2011;22:145–52.
8. Zhang Y, Beck CA, Poletti A, Clement JPt, Prendergast P, Yip TT, et al. Phosphorylation of human progesterone receptor by cyclin-dependent kinase 2 on three sites that are authentic basal phosphorylation sites in vivo. Mol Endocrinol 1997;11:823–32.
9. Clemm DL, Sherman L, Boonyaratanakornkit V, Schrader WT, Weigel NL, Edwards DP. Differential hormone-dependent phosphorylation of progesterone receptor A and B forms revealed by a phosphoserine site-specific monoclonal antibody. Mol Endocrinol 2000;14:52–65.
10. Gass EK, Leonhardt SA, Nordeen SK, Edwards DP. The antagonists RU486 and ZK98299 stimulate progesterone receptor binding to deoxyribonucleic acid in vitro and in vivo, but have distinct effects on receptor conformation. Endocrinology 1998;139:1905–19.
11. Schindler AE, Campagnoli C, Druckmann R, Huber J, Pasqualini JR, Schweppe KW, et al. Classification and pharmacology of progestins. Maturitas 2003;46:S7–S16.
12. Schindler AE, Campagnoli C, Druckmann R, Huber J, Pasqualini JR, Schweppe KW, et al. Classification and pharmacology of progestins. Maturitas 2008;61:171–80.
13. Janzen DM, Rosales MA, Paik DY, Lee DS, Smith DA, Witte ON, et al. Progesterone receptor signaling in the microenvironment of endometrial cancer influences its response to hormonal therapy. Cancer Res 2013; 73:4697–710.
14. Beck CA, Zhang Y, Weigel NL, Edwards DP. Two types of anti-progestins have distinct effects on site-specific phosphorylation of human progesterone receptor. J Biol Chem 1996;271:1209–17.
15. Leonhardt SA, Altmann M, Edwards DP. Agonist and antagonists induce homodimerization and mixed ligand heterodimerization of human progesterone receptors in vivo by a mammalian two-hybrid assay. Mol Endocrinol 1998;12:1914–30.
16. Kim JJ, Kurita T, Bulun SE. Progesterone action in endometrial cancer, endometriosis, uterine fibroids, and breast cancer. Endocr Rev 2013;34: 130–62.
17. D'Souza A, Hinduja IN, Kodali S, Moudgil VK, Puri CP. Interaction of newly synthesized antiprogesterone ZK98299 with progesterone receptor from human myometrium. Mol Cell Biochem 1994;139:83–90.
18. Edwards DP, Altmann M, DeMarzo A, Zhang Y, Weigel NL, Beck CA. Progesterone receptor and the mechanism of action of progesterone antagonists. J Steroid Biochem Mol Biol 1995;53:449–58.
19. Robertson JF, Willsher PC, Winterbottom L, Blamey RW, Thorpe S. Onapristone, a progesterone receptor antagonist, as first-line therapy in primary breast cancer. Eur J Cancer 1999;35:214–8.
20. Huang J, Hu W, Bottsford-Miller J, Liu T, Han HD, Zand B, et al. Cross-talk between EphA2 and BRaf/CRaf is a key determinant of response to Dasatinib. Clin Cancer Res 2014;20:1846–55.
21. Chou TC TP.Quantitative analysis of dose-effect relationships: the combined effects of multiple drugs or enzyme inhibitors. Adv Enzyme Regul 1984;22:27–55.
22. Nishino T, Ishibashi K, Hirtreiter C, Nishino Y. Potentiation of the antitumor effect of tamoxifen by combination with the antiprogestin onapristone. J Steroid Biochem Mol Biol 2009;116:187–90.
23. Yamaguchi T, Kakefuda R, Tajima N, Sowa Y, Sakai T. Antitumor activities of JTP-74057 (GSK1120212), a novel MEK1/2 inhibitor, on colorectal cancer cell lines in vitro and in vivo. Int J Oncol 2011;39:23–31.
24. Bonneterre J, Hutt E, Bosq J, Graham JD, Powell MA, Leblanc E, et al. Development of a technique to detect the activated form of the progesterone receptor and correlation with clinical and histopathological characteristics of endometrioid adenocarcinoma of the uterine corpus. Gynecol Oncol 2015;138:663–7.
25. Arnett-Mansfield RL, Graham JD, Hanson AR, Mote PA, Gompel A, Scurr LL, et al. Focal subnuclear distribution of progesterone receptor is ligand dependent and associated with transcriptional activity. Mol Endocrinol 2007;21:14–29.
26. Moore NL, Edwards DP, Weigel NL. Cyclin A2 and its associated kinase activity are required for optimal induction of progesterone receptor target genes in breast cancer cells. J Steroid Biochem Mol Biol 2014;144:471–82.
27. Shen T, Horwitz KB, Lange CA. Transcriptional hyperactivity of human progesterone receptors is coupled to their ligand-dependent down-regulation by mitogen-activated protein kinase-dependent phosphorylation of serine 294. Mol Cell Biol 2001;21:6122–31.
28. Faivre EJ, Daniel AR, Hillard CJ, Lange CA. Progesterone receptor rapid signaling mediates serine 345 phosphorylation and tethering to specificity protein 1 transcription factors. Mol Endocrinol 2008;22:823–37.
29. Lange CA, Shen T, Horwitz KB. Phosphorylation of human progesterone receptors at serine-294 by mitogen-activated protein kinase signals their degradation by the 26S proteasome. Proc Natl Acad Sci U S A 2000; 97:1032–7.
30. Daniel AR, Qiu M, Faivre EJ, Ostrander JH, Skildum A, Lange CA. Linkage of progestin and epidermal growth factor signaling: phosphorylation of progesterone receptors mediates transcriptional hypersensitivity and increased ligand-independent breast cancer cell growth. Steroids 2007;72:188–201.
31. Qiu M, Olsen A, Faivre E, Horwitz KB, Lange CA. Mitogen-activated protein kinase regulates nuclear association of human progesterone receptors. Mol Endocrinol 2003;17:628–42.
32. Khan JA, Amazit L, Bellance C, Guiochon-Mantel A, Lombes M, Loosfelt H. p38 and p42/44 MAPKs differentially regulate progesterone receptor A and B isoform stabilization. Mol Endocrinol 2011;25:1710–24.

Published OnlineFirst December 13, 2017; DOI: 10.1158/1535-7163.MCT-17-0006

Molecular Cancer Therapeutics

Inhibiting Nuclear Phospho-Progesterone Receptor Enhances Antitumor Activity of Onapristone in Uterine Cancer

Yan Huang, Wei Hu, Jie Huang, et al.

Mol Cancer Ther 2018;17:464-473. Published OnlineFirst December 13, 2017.